AGGREGATION OF SiC-X GRAINS IN SUPERNOVA EJECTA

The Astrophysical Journal, 705:1215–1218, 2009 November 10 doi:10.1088/0004-637X/705/2/1215

AGGREGATION OF SiC-X GRAINS IN SUPERNOVA EJECTA

Ethan A.-N. Deneault
Department of Chemistry and Physics, University of Tampa, Tampa, FL 33606, USA; edeneault@ut.edu
Received 2009 May 7; accepted 2009 August 13; published 2009 October 20

ABSTRACT

We present a model for the formation of silicon carbide aggregates within the expanding and cooling supernova remnant. SiC type-X (SiC-X) grains measured in the laboratory at a high spatial resolution have been found to be aggregates of smaller crystals which are isotopically homogenous. The initial condensation of SiC in the ejecta occurs within an interior dense shell of material which is created by a reverse shock which rebounds from the core–envelope interface. A subsequent reverse shock accelerates the grains forward, but the gas drag from the ejecta on the rapidly moving particles limits their travel distance. By observing the effects of gas drag on the travel distance of grains, we propose that supernova grain aggregates form from material that condensed in a highly localized region, which satisfies the observational evidence of isotopic homogeneity in SiC-X grains.

Key words: supernova remnants – infrared: stars – astrochemistry

1. INTRODUCTION

An important source of interstellar dust is the rapidly expanding and cooling outflows of type II supernovae. Within the highly radioactive interior of the ejecta, Si, C, and O atoms chemically react in an a nearly hydrogen-free environment, forming SiC, CO, and graphite. The most well-studied supernova condensate in the laboratory is the SiC type-X (SiC-X) grains (Clayton & Nittler 2004). Recent studies of the structure and isotopic makeup of these grains (Stroud et al. 2004; Hynes et al. 2006) show that SiC-X grains are typically comprised of an aggregate of smaller isotopically homogenous subgrains—a few tenths of a micron to a micron in size. This microstructure indicates that dust coagulation processes likely occur within the ejecta.

We follow Deneault et al. (2003, hereafter DCH03) in proposing a model for the formation of SiC-X grains in the ejecta, in which SiC will condense in the dense ejecta interior, and be accelerated through the overlying ejecta via reverse shocks. SiC condenses within the dense, hot interior regions of the supernova ejecta. The reverse shock from the core–envelope interface sets up such a high-density region (between 2.7 and 3.6 $M_{\odot}$). Figure 1 reproduces Figure 2 from DCH03 to show the large density enhancement which leads to SiC growth. Although the exact condensation kinetics of SiC within the hydrogen-free supernova interior is currently unknown, there is indication that strong shocks can drive SiC formation (Frenklach et al. 1989). Within the dense region created by the reverse shock, SiC will only form when the Si/C ratio is greater than 10 (DHC03). This condition is satisfied interior to 3.2 $M_{\odot}$ and we consider the region $2.7 < m < 3.2\,M_{\odot}$ to be the primary SiC-condensing region.

The SiC grains' motion is coupled to that of the homologously expanding ejecta initially. A second reverse shock (between 10^7 and 10^9 s after core bounce) caused by the interaction between the fast moving ejecta and the surrounding circumstellar material causes these grains to be decoupled from the gas, and move forward through the overlying material. Recent models of grain survival in ejecta (Nath et al. 2008; Nozawa et al. 2007; Bianchi & Schneider 2007) pose that upward of 20% of the dust mass will be destroyed by sputtering in the reverse shock. Smaller condensates are slowed by the drag force of the gas and non-thermal sputtering and are eventually destroyed by thermal sputtering while larger condensates a few tenths of a micron in size survive roughly intact (Bianchi & Schneider 2007).

Grains that condense farther out in mass coordinate will have a higher velocity than those which condensed closer to the center. Under this expectation, grains will typically not interact. However, DCH03 posed that larger grains formed in inner mass coordinates can overtake smaller grains that formed farther out, because the differential velocity of a grain due to gas drag is proportional to the surface area of the grain. By this method, larger grains would act to sweep up smaller grains in their path. The aggregation model of DCH03 expected that grains of varying isotopic composition would aggregate together. Current evidence (e.g., Nittler et al. 2007) suggests otherwise. Although the nanoscale, intragranular-resolution data on SiC-X grains is limited to a few grains, the available analyses suggest that grain aggregates are formed from subgrains which condensed from a single isotopic reservoir.

2. BALLISTIC MOTION THROUGH THE EJECTA

2.1. Reverse Shocks

The amount of presupernova mass loss determines the timescale for the reverse shock to enter the condensation region as well as the strength of the reverse shock. If the mass loss is too large, the shockwave will enter the condensation region while SiC growth is starting. The high temperatures in the shocked gas will stop condensation within the gas, and the small grains that may have already condensed will be destroyed by thermal and non-thermal sputtering. A reverse shock that arrives within the condensation region after SiC growth has slowed, $t \geqslant 3$ years, is more conducive to grain survival. Decoupled from the gas, larger grains are more apt to survive non-thermal sputtering, and are not melted by the shock (DCH03; Nozawa et al. 2007).

The initial grain velocity depends on where the grain condenses as well as the strength of the reverse shock. The initial grain velocity v_{g0} is the difference between the homologous expansion of the gas and the velocity of the reverse shock. For the purposes of this paper, we take v_{g0} to be a free parameter, and without loss of generality, we choose $v_{g0} = 500$ km s^{-1} to be the "standard" initial velocity, following DHC03.

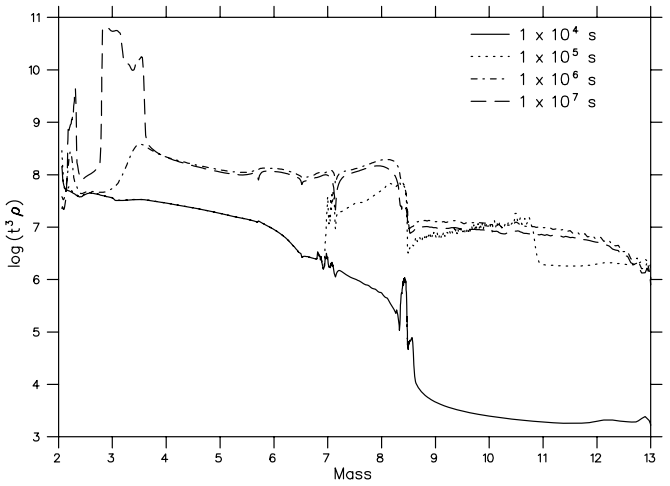

Figure 1. Density of the ejecta in mass coordinate plotted for several different times. The large density enhancement between 2.7 and 3.6 $M_\odot$ contains the SiC condensation region (this figure replicates Figure 2 from DCH03.).

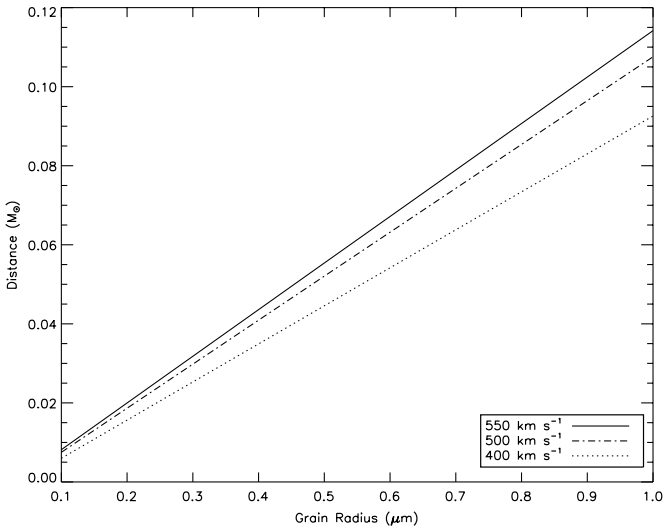

Figure 2. Distance in mass coordinate traveled by grains as a function of grain size for different initial velocities. Smaller grains, regardless of initial velocity remain near their local region, larger grains travel up to 10 times further in mass coordinate.

2.2. Gas Drag

Each grain is decelerated by a drag force which is caused by collisions between the grain and the overlying gas as well as non-thermal sputtering from collisions with gas particles. Non-thermal sputtering serves to erode the dust grain, slowing its forward motion. In this paper, we neglect non-thermal sputtering, and thus provide upper limits to travel distances of grains based on gas drag alone. The grain velocity decreases due to gas drag by Draine & Salpeter (1979):

$$\frac{dv_g}{dt} = -\frac{1}{\rho_g a_g}\left(\frac{3}{2}kT\right)\sum_i n_i G_i(s_i), \quad (1)$$

where a_g is the grain radius, and ρ_g is the density of the SiC grain, and n_i is the number density of species i. The function $G_i(s_i)$ is summed over all gas species

$$G_i(s_i) = \frac{8s_i}{3\sqrt{\pi}}\left(1 + \frac{9\pi}{64}s_i\right)^{1/2}, \quad (2)$$

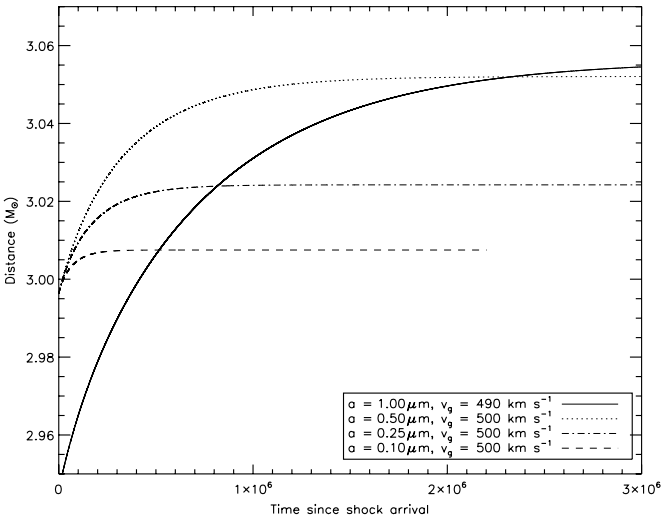

Figure 3. Larger grains formed interior to smaller grains can overtake them. The time axis has been scaled such that zero represents the time when the shock reached the grain. The grain that formed at 2.95 $M_\odot$ can interact with grains up to ~0.50 μm in radius that formed a few hundredths of a solar mass farther out.

and s_i is the atomic speed ratio $s_i = (m_i v_g^2/2kT)^{1/2}$. In this study, as in DCH03, we use the 25 $M_\odot$ ejecta model s25 from Rauscher et al. (2002, hereafter WHW). This is a one-dimensional ejecta model with solar metallicity, and omits instabilities (e.g., Herant & Woosley 1994) that can move inner-ejecta material to higher mass coordinates. The net effect of these instabilities on the ejecta is to move the condensation region for SiC grains to a different mass coordinate, but it does not significantly alter the motion of grains due to reverse shocks, or the condensation chemistry of SiC in these dense clouds.

The effect of the gas drag on the motion of the grain through the overlying ejecta is pronounced. In Figure 2, we show the distance in mass coordinate traveled by the grain as a function of the grain radius and initial velocity through the ejecta. Here, we have assumed the grain begins its motion at 3.0 $M_\odot$ in the s25 model. The total distance traveled is the distance that the grain has moved before the gas drag has slowed the grain enough to be comoving with the gas. Smaller grains are effectively and quickly slowed by the gas drag, slowing to a differential velocity of zero after only a few million seconds, effectively trapping them within a localized region. Larger grains which formed interior to these grains will easily overtake them even though they are moving with a lower initial velocity.

2.3. Grain–Grain Interactions

In Figure 3, we see the path of a hypothetical 1 μm grain formed at 2.95 $M_\odot$. Three other grains which formed in the overlying layer at 2.99 $M_\odot$ are also shown. For clarity, we have not shown grains that may have condensed between those two coordinates. The time axis has been scaled such that zero represents the time when the reverse shock reaches the condensation region of the grain. In the ejecta, the shock reaches the inner zone on the order of 10^7 s later. Although the interior grain has a slower initial velocity, its larger size minimizes the effect of gas drag. In the absence of sputtering or inelastic collisions, the larger grain can travel approximately 0.1 $M_\odot$ in mass coordinate. The velocity of grain collisions decreases with increasing target size, because smaller grains are effectively slowed by gas drag. Low-velocity (thus low kinetic energy) impacts have a much higher chance of grains sticking

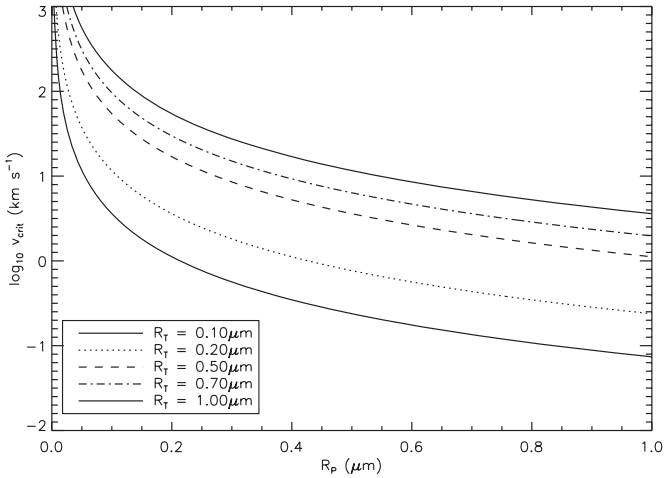

Figure 4. Critical velocity for shattering a target grain as a function of radius of the impacting grain (R_T). Five target radii are plotted from 0.1 to 1.0 μm. Larger SiC grains will shatter smaller grains at even low-speed impacts of a few tenths of a km s^{-1}. Only collisions between similar sized grains at low velocities will lead to aggregation in lieu of shattering.

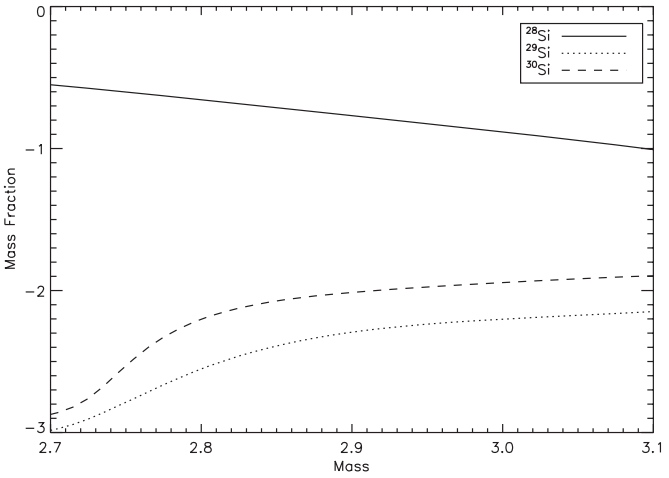

Figure 5. Mass fraction of ^{28,29,30}Si as a function of mass coordinate in the ejecta. We can see that the isotopic composition between 2.8 and 3.1 $M_\odot$ is fairly uniform. Below 2.8 $M_\odot$, the abundances of ^{29,30}Si drop by an order of magnitude. This demonstrates that grains which form near one another will have very similar Si isotopic composition.

and forming aggregates compared with higher velocity impacts, which could shatter the grain (Dominik & Tielens 1997).

Although we have not included grain shattering in the calculation, it is worth considering the effect of grain shattering on the evolution of grains within the ejecta. The critical velocity for catastrophic destruction in a grain–grain collision is given by

$$v_{\rm cat} \propto \left(\frac{R_T^3}{R_P^3}\right)^{9/16}, \quad (3)$$

where R_T and R_P are the target and projectile radii, respectively (adapted from Jones et al. 1996). In Figure 4, we see that small projectiles, less than 0.1 μm need an extremely large relative velocity to shatter a target grain of any size. However, only larger grains can survive catastrophic spallation if the relative velocities between projectile and target are a few km s^{-1}. This implies a very stark picture for the survival of smaller grains. Larger SiC grains which condensed at inner mass coordinate will more likely shatter small grains unless the impact velocity is much less than a km s^{-1}. Aggregates of similar micron-size crystals have been observed in the laboratory (e.g., Nittler et al. 2007). These larger grains are more likely to survive impacts with other similar sized crystals at higher velocities. Figure 4 shows that a 1 μm impactor will not catastrophically shatter a 1 μm target if the velocity is less than about 4 km s^{-1}.

3. CONDENSATE SIZE DISTRIBUTION

Absent any collisions with other grains, a micron-sized SiC grain will travel not much more than 0.2 $M_\odot$ outward before gas drag slows its relative forward motion (compared to the ejecta) to zero. This distance represents a strict upper limit to the motion of the grain in the ejecta. If the condensation region for SiC grains is found between $2.7 < m < 3.2\ M_\odot$ (as discussed in Section 1) that means that SiC grains can interact with material no further than $m = 3.4\ M_\odot$. In the inner region, near 2.7 $M_\odot$, the Si/C ratio approaches 10^4. In this highly Si-saturated region, graphite will be readily converted to SiC (DCH03). Due to the much smaller carbon budget in this region, however, it is very likely that the inner condensation zone will produce both a smaller number of condensates as well as smaller-sized condensates (Deneault et al. 2006). The specific kinematics of SiC formation as a function of the Si/C ratio are unknown, and we do not endeavor to solve this problem in the current paper. As a rule of thumb, we postulate that the size of SiC condensates increases roughly inversely proportional to the Si/C ratio.

As discussed in Section 2.2, the forward motion of small grains is strongly inhibited by gas drag. In the high-temperature postshock environment, thermal sputtering will efficiently destroy small grains. Since the interior condensation region produces only these smaller grains, aggregate formation is essential for SiC grain survival in this region. Because a smaller number of initial condensates are formed, however, aggregates from the interior region will be rare, and comprised primarily of smaller subgrains. Similarly, the Si/C ratio drops below 10 above 3.25 $M_\odot$, which inhibits the growth of SiC. Grains which condensed near this outer edge of the region will not form SiC aggregates with overlying material, and will remain single crystals. The central region of the condensation zone, between 2.9 and 3.1 $M_\odot$, is the most likely place for aggregate formation.

4. ISOTOPIC COMPOSITION OF GRAINS

DCH03 proposed that an aggregate of grains would have a noticeable isotopic heterogeneity, in which each subgrain of the aggregate would have a markedly different isotopic composition. Laboratory studies of presolar aggregates show that such isotopic heterogeneity is rare (Besmehn & Hoppe 2002; Nittler et al. 2007), although not unknown. We believe that the observed isotopic homogeneity of supernova aggregates indicates that the process of coagulation occurs in a highly localized area of the ejecta. Due to gas drag, the travel distance of a grain is limited. It will only have the chance to interact and coagulate with grains that formed nearby. As discussed in Section 2.3, large grains, which decelerated the least by gas drag will have only limited capability of interacting with overlying grains, smaller grains, much less so.

Does this interior region produce the ^{28}Si excess observed in SiC-X grains? As we can see in Figure 5, the condensation and aggregation region between 2.9 and 3.1 $M_\odot$ does have a substantial ^{28}Si excess. This excess varies by a factor of 3 over the region, but is always at least a factor of 10 higher

than the abundances of ^{29,30}Si. If we consider the supernova to be of half-solar metallicity (as per DCH03), the ^{28}Si abundance will be much higher in this region. The Si isotopic ratios are consistent with what is found in the observed grains. The $^{14}N/^{15}N$ ratio, however, is near 1.6×10^{-2} within the same region. This is far lower than the measured ratio in X grains, which sits between 20 and 200 (Hoppe et al. 2000). DCH03 proposed that the implantation of ^{14}N would occur as the grain is propelled through the ejecta, but implantation is insufficient to overcome this problem even if the grain is allowed to travel through the complete ejecta. The $^{26}Al/^{27}Al$ ratio is also much smaller than observed. Although the 25 $M_{\odot}$ ejecta model that we have used in this paper does not consider the possibility of mixing of gases in the ejecta (e.g., Yoshida 2007), it may be necessary to consider. If the ejecta is mixed before the grains condense, we can overcome the difficulties present in the implantation model of DCH03 for short travel distance.

5. EJECTION INTO THE INTERSTELLAR MEDIUM (ISM)

The rapidly decreasing grain velocities in our model effectively retard the total distance which grains can travel relative to the gas. This poses a severe problem, as the grains will remain effectively trapped within the expanding ejecta, and not ejected into the ISM. We propose that the grains will be ejected into the ISM by a third reverse shock between the outward moving ejecta and the ISM. The time for this reverse shock is much longer (10^9–10^{11} s) than that of the previous shock due to the circumstellar material. We predict that at these late times, the ejecta will be very diffuse and the accelerated grains will not be slowed appreciably by the gas drag or by sputtering, allowing them to emerge into the ISM.

6. CONCLUSION

In this paper, we have presented a model for the aggregation of SiC grains in the supernova interior. In the one-dimensional model, SiC will condense within a limited region of the interior where the number density of Si atoms is greater than 10 times that of C. When the reverse shock passes through the condensation region, the grains are decelerated much less than the surrounding gas, and they ballistically move through the overlying ejecta. Gas drag from the ejecta slows these grains down with a rate inversely proportional to the radius of the grain. Larger grains can shatter smaller grains through impacts, but grains that have low relative velocities can aggregate together. The gas drag highly truncates the distance which a grain can travel, thus an aggregate will likely be comprised only of grains with similar isotopic composition.

We have not set out in this work to show a detailed kinetic description of grain coagulation within the ejecta, but rather to provide a more refined physical model for that process beyond what was hypothesized in DCH03. The greatest uncertainty in this model is whether grains will actually coalesce in the low-speed ballistic collisions that we have presented, and what effects those collisions have on the evolution of the aggregate grain. We have also omitted the effects of sputtering and turbulent motion of the ejecta on the grains' travel. Future ongoing work in this area will provide us with a more complete picture of the processes of SiC dust aggregation within the ejecta.

The author thanks Larry Nittler for his helpful correspondence.

REFERENCES

Besmehn, A., & Hoppe, P. 2002, Lunar and Planetary Institute Conference Abstracts, 33, 1297
Bianchi, S., & Schneider, R. 2007, MNRAS, 378, 973
Clayton, D. D., & Nittler, L. R. 2004, in As part of the Carnegie Observatories Astrophysics Series, Origin and Evolution of the Elements, from the Carnegie Observatories Centennial Symposia, ed. A. McWilliam & M. Rauch (Cambridge: Cambridge Univ. Press), 300
Deneault, E. A.-N., Clayton, D. D., & Heger, A. 2003, ApJ, 594, 312
Deneault, E. A.-N., Clayton, D. D., & Meyer, B. S. 2006, ApJ, 638, 234
Dominik, C., & Tielens, A. G. G. M. 1997, ApJ, 480, 647
Draine, B. T., & Salpeter, E. E. 1979, ApJ, 231, 438
Frenklach, M., Carmer, C. S., & Feigelson, E. D. 1989, Nature, 339, 196
Herant, M., & Woosley, S. E. 1994, ApJ, 425, 814
Hoppe, P., Strebel, R., Eberhardt, P., Amari, S., & Lewis, R. S. 2000, Meteorit. Planet. Sci., 35, 1157
Hynes, K. M., Croat, T. K., Amari, S., Mertz, A. F., & Bernatowicz, T. J. 2006, Meteoritics & Planetary Science Supplement, 41, 5333
Jones, A. P., Tielens, A. G. G. M., & Hollenbach, D. J. 1996, ApJ, 469, 740
Nath, B. B., Laskar, T., & Shull, J. M. 2008, ApJ, 682, 1055
Nittler, L. R., Hoppe, P., & Stroud, R. M. 2007, in Lunar and Planetary Institute Conference Abstracts, 38, 2321
Nozawa, T., Kozasa, T., Habe, A., Dwek, E., Umeda, H., Tominaga, N., Maeda, K., & Nomoto, K. 2007, ApJ, 666, 955
Rauscher, T., Heger, A., Hoffman, R. D., & Woosley, S. E. 2002, ApJ, 576, 323
Stroud, R. M., Nittler, L. R., & Hoppe, P. 2004, Meteoritics & Planetary Science Supplement, 39, 5039
Yoshida, T. 2007, ApJ, 666, 1048